Journal of Building Engineering 88 (2024) 109191

Contents lists available at ScienceDirect

Journal of Building Engineering

journal homepage: www.elsevier.com/locate/jobe

A comprehensive analysis of hydration kinetics and compressive strength development of fly ash-Portland cement binders

Rohan Bhat [a], Taihao Han [a, *], Gaurav Sant [c], Narayanan Neithalath [b], Aditya Kumar [a]

[a] Department of Materials Science and Engineering, Missouri University of Science and Technology, Rolla, MO, 65409, USA
[b] School of Sustainable Engineering and the Built Environment, Arizona State University, Tempe, AZ, 85287, USA
[c] Civil and Environmental Engineering, University of California, Los Angeles, Los Angeles, CA, 90095, USA

ARTICLE INFO

Keywords:
fly ash
Sustainable cementitious binder
Compressive strength
Hydration kinetics
Reactivity
Phase assemblage

ABSTRACT

Utilizing fly ash (FA) to partially replace Portland cement (PC) in formulating sustainable cementitious binders can significantly mitigate environmental impacts associated with PC manufacturing and improper disposal of FAs. The main objective of this research is to employ a cost-efficient and simple method to assess the reactivity of FAs in PC. This is intended to enhance the replacement level of FAs in PC, without scarifying its performance. In this study, 10 FAs—each with unique chemical composition and molecular structure—are used to substitute two PCs at 10-to-50%$_{mass}$ replacement levels. Hydration kinetics and compressive strength of [PC + FA] binders are investigated. Equilibrium phase assemblages obtained from thermodynamic simulations were used to estimate the volume fraction of hydrates formed in [PC + FA] binders. The correlation between compressive strength of [PC + FA] binders and their volume fraction of hydrates is explored and employed to determine the degree of reaction of FA. The *number of constraints* derived from the topological constraint theory are used to represent the reactivity of FAs. Outcomes indicate that FAs with low value of *number of constraints* tend to show, resulting in enhanced hydration heat release and improved compressive strength. This improvement occurs irrespective of PC composition and replacement level of FA. The reactivity of FA ranges from 3 % to 29 % at 3 days.

1. Introduction

Coal serves as one of the most major sources of energy worldwide. It currently contributes to over 37 % [1] of global electricity production. However, in recent past, there has been a notable shift towards renewable energy sources, resulting in a corresponding decrease in the usage of coal. Despite this shift, it is projected that by 2040, coal will still be accountable for approximately 22 % [2] of the electricity generated worldwide. Despite this trend, many Asian countries, such as China, continue to increase their coal consumption. For instance, the primary coal demand in China is projected to grow from 1308 million tons in 2002–2402 million tons in 2030 [3,4]. However, this extensive consumption of coal comes with significant environmental implications, particularly in the form of waste by-products. One of the most substantial by-products of coal combustion is coal ash, which includes fly ash (FA) and bottom ash. These ashes are the solid remnants of the burnt coal, with the lighter FA being carried off in the flue gas and the heavier bottom ash settling at the bottom of the furnace. Globally, the production of fly and bottom, with an estimated 800 million tons produced annually [5,6]. Forecasts suggest that this trend will continue, with global FA production set to surpass 1.04 billion tons by 2030 [7]. The recycling and utilization of this coal ash vary widely across the world. Utilization rates range from a low of 3 % to as high as 90 %

* Corresponding author. Department of Materials Science and Engineering, Missouri University of Science and Technology, 248A McNutt Hall, 1400 N Bishop, Rolla, MO, 65409, USA.
E-mail address: thy3b@mst.edu (T. Han).

https://doi.org/10.1016/j.jobe.2024.109191
Received 18 October 2023; Received in revised form 19 March 2024; Accepted 29 March 2024
Available online 8 April 2024

in different countries [8]. According to research [9], the United States has a FA utilization rate of 50 %, while the European Union surpasses this with a rate of over 90 %. India and China have utilization rates above 60 %. Despite these promising utilization rates in some parts of the world, the global average remains low, having increased from 16 % to a mere 25 % of the total ash produced [8,10,11]. This data highlights that a substantial proportion of coal ash is simply discarded into landfills. This mismanagement of coal ash is prevalent in numerous parts of the world and poses a considerable risk to the environment. The ash can infiltrate the subsoil, contaminating groundwater with heavy metals and leading to various environmental issues, both in the past and in the future [12–14]. The disposal of FA in landfills can also lead to the release of harmful gases such as methane and carbon dioxide [15–17]. These gases contribute to the greenhouse effect and contribute to global warming, which has severe implications on the environment. Another significant drawback associated with the disposal of FAs is their contribution to chronic health issues in both humans and animals, stemming from the heavy metals in them. The contamination of vegetation by such waste materials has been linked to severe health concerns (e.g., cancer, liver complications, neurological disorders, etc.) [18]. This correlation underscores the criticality of addressing the mishandling and improper disposal of FAs. A recent study [19] has demonstrated the importance of effective waste management practices for FAs to mitigate their adverse environmental impacts. Furthermore, this research highlights the inherent safety and user-friendliness of FAs, owing to their potential antimicrobial properties, when managed properly. Thus, it becomes crucial to prioritize the recycling and utilization of coal ash to mitigate its environmental impact.

Portland cement (PC) is the most widely used human-made material in construction, with a global annual production of over 4 billion tons. However, the production of this ubiquitous material comes with a substantial environmental cost. It is responsible for approximately 4–9% of anthropogenic CO_2 emissions [20–22]. This considerable carbon footprint is largely due to the decarbonation of limestone and the calcination of raw materials at very high temperatures. Given the expected increase in global population, which is estimated to be around 82 million yearly [23], the applications of PC continually grow, further exacerbating greenhouse gas emissions. In response to this pressing environmental issue, the International Energy Agency and World Business Council for Sustainable Development have proposed various roadmaps to conserve energy and substantially reduce CO_2 emissions in the cement industry [24,25]. In alignment with these roadmaps, the cement industry has undertaken measures to improve energy efficiency. This includes the adoption of renewable energy, CO_2 capture, and more efficient manufacturing processes [26–28]. However, these efforts are not sufficient to meet the CO_2 reduction target, and thus, additional options for reducing cement demand must be explored. To further improve the sustainability of the cement industry, partial replacement of PC with FA is currently the most practical solution, while also maintaining good mechanical properties and durability. This application offers a dual benefit by not only reducing the amount of FA that ends up in landfills, which negatively impacts the environment, but also contributing to a reduction in CO_2 emissions from the PC industry. This dual benefit approach has the ability to make a considerable contribution to global efforts to alleviate the effects of climate change, as well as encourage sustainable waste management practices.

FAs demonstrate substantial batch to batch heterogeneity in their chemical compositions, which are attributed to differences in upstream coal sources, combustion technologies, cooling processes, and collection methodologies. This inconsistency in composition stands in stark contrast to other Supplementary Cementitious Materials such as quartz, silica fume, metakaolin, etc. FAs comprise of CaO (C), SiO_2 (S), Al_2O_3 (A), SO_3 ($), and other metal oxides abbreviated based on cement chemistry. FAs participate in the hydration of PC through two key reaction mechanisms. Firstly, the silicate ions from FAs participate in a pozzolanic reaction by reacting with portlandite (CH, H_2O abbreviated as H)—a secondary hydration product—to produce C–S–H [29]. Secondly, FAs offer additional surfaces for the heterogeneous nucleation and growth of C–S–H, an effect commonly referred to as the filler effect [30,31]. Unlike other Supplementary Cementitious Materials, the distinctive presence of SO_3 in FA facilitates reactions with highly reactive C_3A, producing ettringite in the early stages, and monosulfoaluminate coming after ages. The amorphous phase contents of FAs generally vary between 50 and 90%$_{mass}$, causing their reactivity to span over a wide range. FAs are broadly classified into two types based on ASTM C618 [32]: Class-C, where the FA comprises more than 18 % CaO; and Class-F, where the FA contains less than 18 % CaO. Nevertheless, multiple studies have suggested that this classification doesn't adequately present the reactivity of FAs. Previous research has demonstrated that the Topological Constraint Theory (TCT) is a simple but effective method to estimate the reactivity of FAs. Based on the topology of atomic structures in the amorphous phases of FAs, the TCT simplifies the complexities associated with amorphous materials into a single parameter: "*number of constraints* (n_c)". It estimates the reactivity of FAs based solely on the content of three major oxides present in the FAs (i.e., C, S, and A) as determined by X-Ray Fluorescence (XRF). Our previous studies [33,34] have evidenced that n_c is an excellent indicator to represent the reactivity of FAs.

Previous studies [35–42] have focused on developing sustainable cementitious binders using FAs. These investigations primarily delved into the hydration kinetics and subsequent microstructural evolution of the [PC + FA] binders. While these studies have shed light on various aspects of the interactions between PC and FA, they have not provided a comprehensive understanding of the underlying influences of FAs, particularly in terms of their chemical composition and molecular structure, on the hydration kinetics and microstructural development of cementitious binders. This is because the reactivity of FAs was ignored. As previously noted, even FAs that exhibit similar compositions can manifest disparate behaviors during the hydration reaction due to their distinct reactivity and molecular structures. Several studies have shown that the reactivity of FAs in cementitious binders can be measured by the following methods. Haha et al. [43], used different techniques to determine the reactivity of FA such as selective dissolution, dissolution of FA in a diluted alkaline solution and image analysis. Glosser et al. [44], presented a model to quantify the dissolution of glassy phases in fly ashes. Li et al. [45], quantitatively determined the anhydrous FA in hydrated cement-FA binders using selective dissolution, X-ray diffraction and energy-dispersive X-ray analysis. These studies have used very complex and expansive techniques to evaluate the reactivity of FAs, which cannot be accessed by many researchers. It is valuable to employ a simple method to discover the reactivity and performance of FA in PC. Moreover, previous research has predominantly focused on a single type of PC, coupled with a limited type

of FA, usually one or two at most. This has subsequently led to an incomplete understanding of the influence from FA with various chemical compositions and molecular structures of FAs on PC hydration and microstructure development.

In this study, ten FAs possessing different chemical compositions and molecular structures are employed to partially substitute two PCs at 10-to-50%$_{mass}$. This study decodes the calorimetry results of [PC + FA] binders to gain a comprehensive understanding of how FAs influence the hydration kinetics of PC. Furthermore, this study also explores the impact of FAs on the mechanical properties (i.e., compressive strength) of [PC + FA] binders. This includes uncovering the correlations between the compressive strength, FA replacement level, and reactivity (i.e., *number of constraints*). In addition, thermodynamic simulations are utilized to develop the phase assemblages of [PC + FA] binders. By combining these phase assemblages with the measured compressive strength, the degree of reaction of FA in each binder is evaluated. Subsequently, the degree of FA reaction is correlated with the *number of constraints* to assess the effectiveness of these constraints in estimating the reactivity of FA. This is a first study use a broad range of FAs with varied chemical compositions and structures to explore their influence on hydration kinetics and mechanical properties. This provides a comprehensive guideline for researchers to select FAs for the development of sustainable cementitious binders. Additionally, it introduces an innovative methodology, combining thermodynamic simulation and compressive strength measurement, to evaluate the reactivity of FAs.

2. Experimental methods

This study utilized 10 fly ashes (FA-1-to-10, supplied by Boral Resources, USA) to partially replace two Type I/II PCs (PC-1 and PC-2, supplied by Boral Resources, USA). The phase composition, chemical composition, and specific surface area of PCs and FAs are presented in Table S1 and Table S2, respectively. The TCT was used to derive the *number of constraints* (shown in Table S2) for all FAs using the main oxides (i.e., C, S, and A). The *number of constraints* consolidates the chemical structure and reactivity of FAs into one singular chemo-structural parameter. Based on their chemical compositions, FAs used in this study can be classified into: partially depolymerized regime (high reactivity) and fully polymerized regime (low reactivity). Isothermal calorimetry was used to record the hydration kinetics of [PC + FA] binders, and the compressive strength at 3 days was tested based on ASTM C109 [46]. Thermodynamic simulations encompassing all the [PC + FA] binders were obtained using the Gibbs Energy Minimization software (GEMS) [47], simply based on the bulk chemical composition, liquid-to-solid ratio, and curing temperature. Additional details about experimental methods, topological constraint theory, and thermodynamic simulations can be found in **Supplementary Information**.

3. Results and discussions

3.1. Hydration kinetics

Isothermal calorimetry measured the heat evolution profiles for [PC-1 + 30%FA] binders over 72 h (shown in Fig. 1). Similar hydration behaviors were observed for [PC-2 + 30%FA] binders. Both cumulative heat release and heat flow rates were normalized per gram of cement. The 30 % replacement level was chosen as it adequately demonstrated the influences of FA on cement hydration without dominating the hydration reaction. As aforesaid, FAs can physically and chemically influence hydration kinetics, depending on their chemical compositions and molecular structures. Therefore, the hydration kinetics were divided into two categories based on the types of FA (i.e., partially depolymerized, and fully polymerized). Previous studies [48–50] have shown that depending on the chemical composition and structure, FAs can either accelerate or retard the hydration reaction.

As depicted in Fig. 1a and **b**, the early age hydration of PC is slowed down by replacing PC with partially depolymerized FAs, where hydration peaks occur later in comparison to those observed in plain PC. Partially depolymerized FAs, which have a higher amorphous content, could exhibit great solubility and reactivity in solutions, leading to the release of a large abundance of ions (i.e., SO_4^{2-}, $Al(OH)_4^-$, and $H_2SiO_4^{2-}$). Previous studies [29,51] have shown $Al(OH)_4^-$ absorbs on the topological sites of cement particles, inhibiting water contact and consequently suppressing the hydration process. As is known, C_3A reacts instantaneously with water to form hydrogarnet. To retard this reaction, gypsum is added to PC, resulting in the formation of ettringite and monosulfoaluminate [52]. However, an excessive amount of SO_4^{2-} ions can substantially prolong the induction period. $H_2SiO_4^{2-}$ released from FAs can react with free lime present in the solution, leading to the formation of additional hydrates and the release of more heat. These are the reasons for the induction periods of all partially polymerized binders are longer than the plain binder. By comparing the heat flow rate profiles of [PC-1 + FA-1] and [PC-1 + FA-7] in Fig. 1a, [PC-1 + FA-7] shows a sharper decline in heat flow rate following the hydration peak. Although both FAs have similar compositions, especially A content, FA-7 is more reactive because FA-7 has the lowest mean particle size (d50–7.45 μm) amongst all partially depolymerized FAs and releases a higher amount of $Al(OH)_4^-$. This observation reinforces the notion that $Al(OH)_4^-$ suppress the hydration reaction. As a result, less amounts of hydrates are formed, causing the [PC + FA-7] to release less heat than plain PC. This explanation also accounts for the lower cumulative heat release observed in the [PC + FA-8]. In Fig. 1b, it is observed that [PC-1 + FA-7] shows a much lower cumulative than plain binder and other partially depolymerized FA binders. FA-7 has the highest A content among all partially depolymerized. Therefore, a high amount of $Al(OH)_4^-$ can be released to the pore solution. Excessive $Al(OH)_4^-$ prevents cement particles to contact water, resulting in a slow hydration reaction. Whereas [PC-1 + FA-6] exhibits the highest cumulative heat release. FA-6 has the lowest *number of constraints* (n_c = 3.28), which implies a high solubility of ions. Therefore, a strong pozzolanic reaction is expected to occur. Additionally, $ content in FA-6 is the highest among all partially depolymerized FAs, enabling $ to react with C_3A and form excessive ettringite and monosulfoaluminate. The formation of ettringite and monosulfoaluminate produces more heat than the hydrogarnet formation [53–55].

Fig. 1c and **d** illustrate the heat flow rate and cumulative heat profiles over a 72-h period for binders that have partially replaced PC with fully polymerized FAs. Owing to their high crystalline content, fully polymerized FAs release ions gradually. It can be ex-

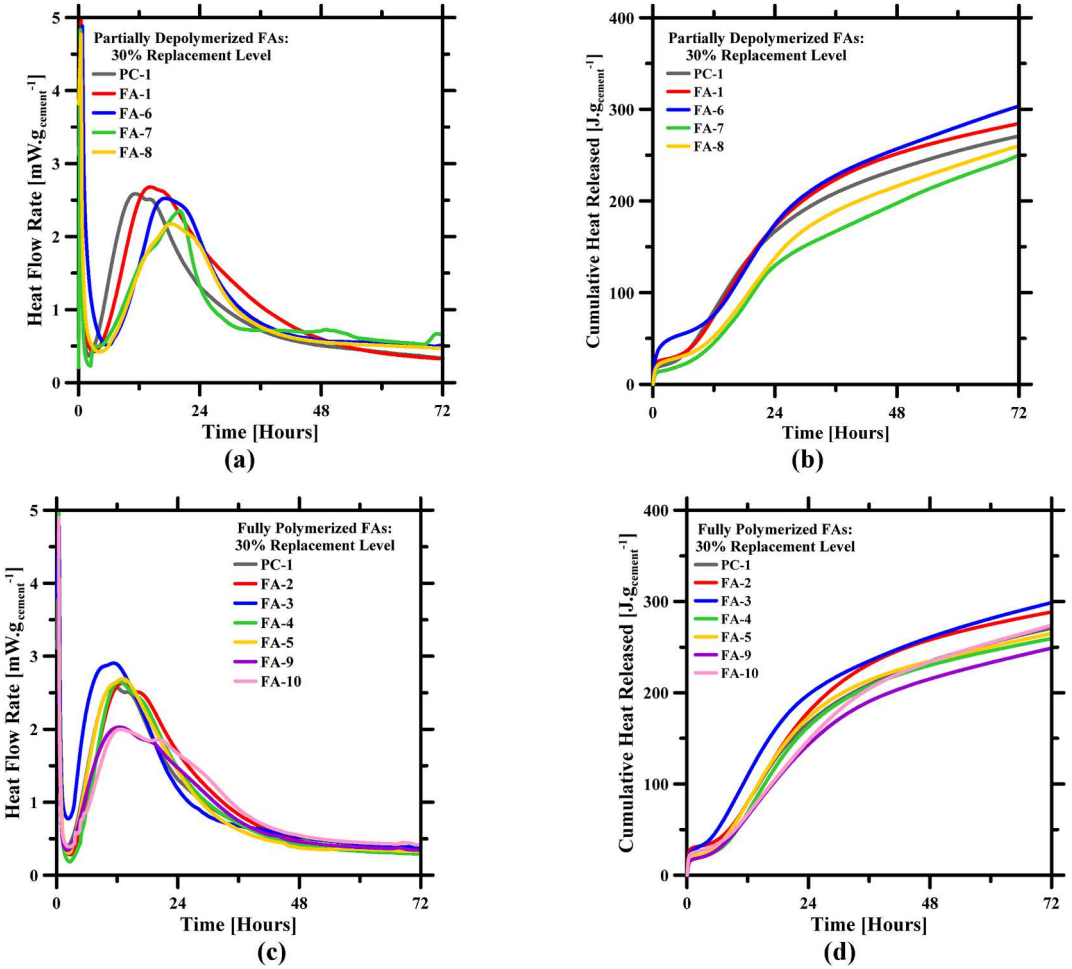

Fig. 1. Heat evolution profiles of [PC-1 + 30 % FA] binders: **(a)** heat flow rate substituted by partially depolymerized FAs; **(b)** cumulative heat substituted by partially depolymerized FAs; **(c)** heat flow rate substituted by fully polymerized FAs; and **(d)** cumulative heat substituted by fully polymerized FAs. Heat evolution profiles were recorded by isothermal calorimetry over 72 h. The FA type is shown in the legend.

pected that fully polymerized FAs perform more physical influence on hydration kinetics than partially depolymerized FAs. As observed in Fig. 1c, fully polymerized FAs tend to reduce the induction period of PC, resulting in a sharp incline during the acceleration phase until the primary hydration peak is reached. This phenomenon can be attributed to the filler effect, where fully polymerized FAs provide additional surfaces for the nuclei of hydrates to grow. FA-3 demonstrates a unique behavior compared to other fully polymerized FAs. [PC-1 + FA-3] exhibits the highest intensity of heat flow peak, the shortest induction period, and the most substantial heat release. FA-3 contributes to this high heat flow peak via two mechanisms. First, FA-3 has little-to-no $ content, and hence its influence can be disregarded. Although FA-3 has low solubility, its high S content (77.1 % mass) ensures that sufficient $H_2SiO_4^{2-}$ ions are released into the solution, thereby causing an intense pozzolanic reaction. Second, amongst all low-Ca FAs, FA-3 had the lowest particle size (d50–8.69 μm) resulting in the highest specific surface area, providing additional surfaces for the heterogeneous nucleation and growth of C–S–H and thus, resulting in the highest heat flow peak. In Fig. 1d, despite the strong filler effect, it is surprising that PC with fully polymerized FA exhibit similar cumulative heat release compared to plain PC. This can be explained by the fact that small amounts of released $Al(OH)_4^-$ released from FAs compensate for the filler effect. It is also worth noting that [PC-1 + FA-2] release significantly more heat than the hydration reaction of plain PC. This occurs because FA-2 is the most inert FA – with the highest n_c value – and contains the highest content of $ (~4 %). Consequently, the filler effect predominantly influences PC hydration, while the increased heat release can be attributed to the consumption of $ resulting in the precipitation of ettringite and monosulfoaluminate. [PC-1 + FA-9] binder, has the lowest cumulative heat released amongst all fully polymerized FAs. This can be attributed to the fact that FA-9 has the second highest *number of constraints* value resulting in a rigid structure and low intrinsic ion dissolution rate. Even though FA-9 has sufficient amount of S (63.1 % mass) to ensure sufficient $H_2SiO_4^{2-}$ are released into the solution, the A content in FA-9 is the highest amongst all fully polymerized FAs, thereby resulting in the lowest cumulative heat. Upon comparing the hydration kinetics between cement replaced by partially depolymerized FA (i.e., [PC-1 + FA-6]) and fully polymerized FA (i.e.,[PC-1 + FA-3]), it is clear that FA-6, releases substantial amounts of ions in the solution allowing the formation of PC hydrates due to the low rigidity of their topological structure. While FA-3, a fully polymerized FAs, provides additional surfaces for the heterogenous nucle-

ation and growth of PC hydrates showing a predominant filler effect which can be observed by shortening of the induction period, leftward shift in the heat flow peak, and the highest intensity of the heat flow peak.

After acknowledging the impacts of the chemical composition and reactivity of FAs on the hydration of PC, it is equally crucial to understand the influence of FA content. Fig. 2 illustrates the effect of FA content on the hydration kinetics of PC-2, utilizing the heat evolution profiles of [PC-1 + FA-9] at five replacement levels. Notably, the hydration behaviors were found to be similar to the selected binder. In [PC-2 + FA-9] binder, FA-9 was chosen as the representative FA due to its rich aluminosilicate composition and negligible $ content (~0.63 %). As the FA-9 content increases, the filler effect becomes substantially more pronounced in PC hydration. This results in a leftward shift of the heat flow rate, a steeper slope for the hydration peak, and a shortening of the induction period. Additionally, elevated levels of FA-9 replacement result in a higher abundance of nucleation sites for the heterogeneous nucleation of C–S–H. This is further evidenced by the intensified hydration peak and the increased cumulative heat, indicating a substantial enhancement in the kinetics of C–S–H precipitation at these replacement levels.

The effect of FAs on the hydration kinetics of both PC-1 and PC-2 are similar, wherein the fully polymerized FAs shorten the induction period, provide additional surfaces for heterogenous nucleation and growth of C–S–H due to the filler effect. Whereas, partially depolymerized FAs, due to a less rigid structure, release more ions (e.g., $H_2SiO_4^{2-}$; $Al(OH)_4^-$; Ca^{2+}; SO_4^{2-}; etc.) into the pore solution and showed a greater contribution towards the pozzolanic reaction.

3.2. Compressive strength

The compressive strength of [PC + FA] binders was measured at 3 days, and Fig. 3 shows the relationship between compressive strength and cumulative heat release. Herein, the unit for cumulative heat is J. g_{water}^{-1} instead of J. g_{cement}^{-1} because normalizing the cumulative heat by the initial water content accounts for the capillary porosity in the binders. Compressive strength is not solely a function of solid-to-solid connectivity within PC but is also related to capillary porosity [56–60]. Numerous studies [31,61–64] have demonstrated that compressive strength is broadly correlated with cumulative heat (normalized by water content) in PC binders, generally in a linear manner. As depicted in Fig. 3, compressive strength increases monotonically with increasing cumulative heat encompassing all [PC + FA] binders investigated in this study. The compressive strength of [PC + FA] binders falls within the range of 15–45 MPa at 3days, aligning with standard performance range of cementitious materials [65–67]. This linear trend emerges because greater cumulative heat entails a higher degree of hydration, leading to the formation of a substantial amounts of hydrates, high solid-to-solid connectivity, and minimal porosity. Hence, the high degree of hydration leads to high compressive strength. The compressive strength of the [PC + FA] binders is inversely proportional to the replacement level. Although FAs can form hydrates through the pozzolanic reaction, the impact on compressive strength is insignificant due to the relatively low intensity of this reaction. In this context, FAs can be considered similar to aggregates, which, as a previous study [68] has shown, can decrease the compressive strength of concrete when their proportion is increased.

As previously mentioned, FAs show an insignificant impact on compressive strength by comparing the replacement levels. However, at the same replacement level, the compressive strength of [PC + FA] binder is related to chemical composition and reactivity of FAs. Fig. 4 demonstrates the relationship between the compressive strength of [PC + FA] and the reactivity (*number of constraints*) of FAs at the same replacement level. Fig. 4a and b represent PC-1 and PC-2 substituted by partially depolymerized FA. As observed earlier in **Section 3.1**, these partially depolymerized FAs are expected to release a large amount of ions (e.g., $H_2SiO_4^{2-}$; $Al(OH)_4^-$; SO_4^{2-}; etc.) into the solution, enabling them to participate in the pozzolanic reaction. Their ability to consume portlandite leads to the formation of additional strength-providing hydrates, thus increasing compressive strength [69]. As a result, the general trend indicates that higher reactivity (lower n_c) of FAs contributes to increased compressive strength. However, FA-6 (n_c = 3.28) slightly deviates

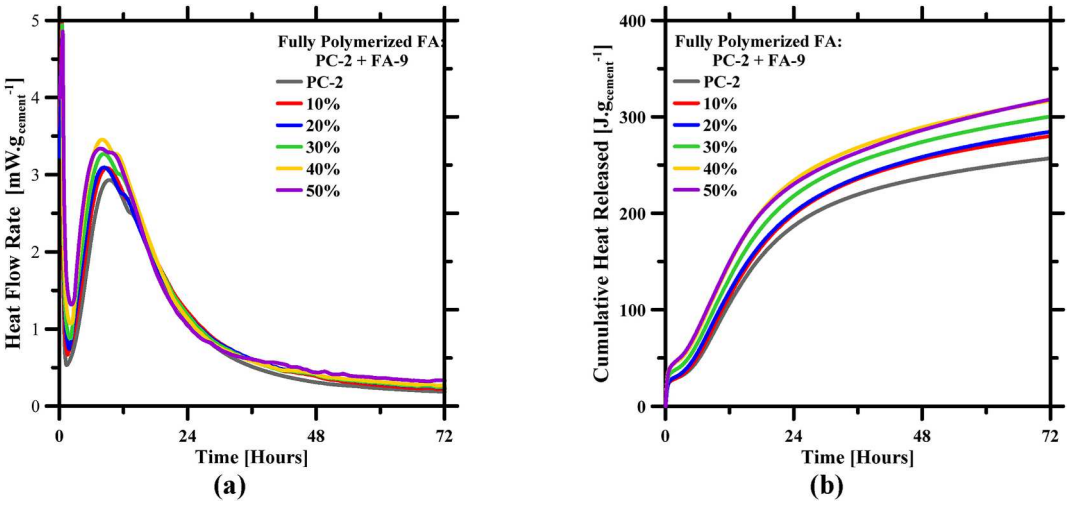

Fig. 2. Heat evolution profiles of [PC-2 + FA-9] binders: **(a)** heat flow rate and **(b)** cumulative heat profiles at various replacement levels. The replacement levels of FA-9 are shown in the legends. Heat evolution profiles were measured by isothermal calorimetry over 72 h.

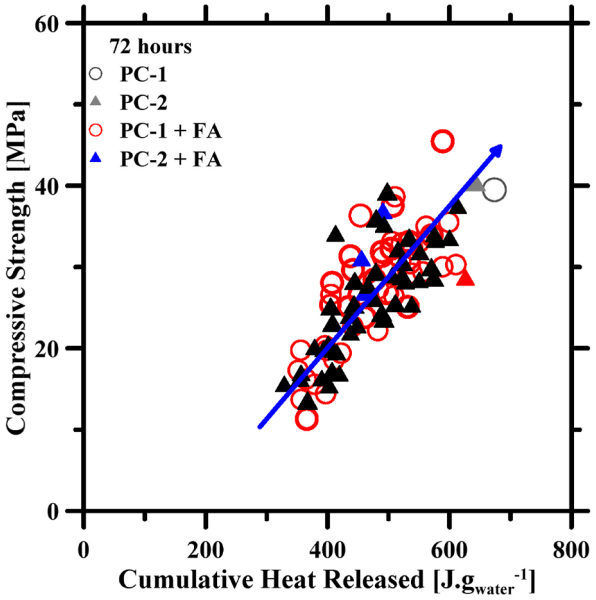

Fig. 3. Correlations between compressive strength and cumulative heat (J. g_{water}^{-1}) at 3 days. The solid blue line represents the trend of the correlation.

from this trend due to its low S content. Although it releases a substantial number of ions into the solution, the intensity of the pozzolanic reaction is not sufficient to enhance the compressive strength. As shown in Fig. 4c and d, the compressive strength of [PC + FA] binders further decrease as the FAs' *number of constraints* increases (low reactivity). This is because fully polymerized FAs have a more rigid, networked structure, making them less reactive and unable to participate in pozzolanic reactions that would promote the formation of strength-providing hydrates. Also, the prominent filler effect observed in fully polymerized FAs provide substantial sites for the heterogeneous nucleation and growth of PC hydrates, thereby only demonstrating an accelerated effect on PC hydration which has been confirmed previously [70]. Consequently, binders replaced by partially depolymerized FAs exhibit higher compressive strength than those replaced by fully polymerized FAs. Overall, the trend observed in both [PC + FA] binders indicates that, regardless of the composition of PC and the replacement level of FAs, the compressive strength of [PC + FA] decreases with an increase in the *number of constraints* of FAs.

3.3. FA reactivity estimation

The previous section demonstrated that FAs could influence the compressive strength of cementitious binders. To further understand the role played by FAs, it is essential to understand their reactivity of FAs at 3 days. This section uses the thermodynamic simulation and compressive strength to evaluate the reactivity of FAs. The thermodynamic simulations were performed using GEMS, based on the mixture design provided as the bulk chemical composition, liquid-to-solid ratio, and curing temperature. The thermodynamic simulation produces phase assemblages of plain PCs, which are presented in Fig. 5. The major phases include C–S–H, portlandite, ettringite, and monosulfoaluminate. Similar simulation results are shown in previous research [42,49]. These phase assemblages provide insight into the volume fraction of hydrates and anhydrate precursors in relation to the degree of hydration of PC. The volume fraction of hydrates is particularly useful for estimating compressive strength, as it is a direct metric to present the solid-to-solid connectivity within the cementitious binders. The degree of hydration for plain PC-1 and PC-2 is estimated to be 50.65 % and 53.53 % at 3 days, respectively. The degree of hydration for both PCs is evaluated using the ratio of short- and long-term calorimetry experiments. Here, the ratio of cumulative heat at 3 days–21 days is considered, with the assumption that PC-1 and PC-2 are fully reacted at 21 days [29]. Fig. 5a and b exhibit the volume fraction of hydrates with respect to the degree of hydration for PC-1 and PC-2. It is worth noting that the strength-providing phase (i.e., C–S–H) is more abundant in PC-2 than in PC-1. The volume fraction of C–S–H in PC-1 at 3 days is 0.244, while that of PC-2 is 0.275. This difference arises because PC-2 has a higher degree of hydration than PC-1. This has also been observed in the measured compressive strength of PC-1 and PC-2 at 3 days: PC-1 has a compressive strength of 39.51 MPa, while PC-2's compressive strength is 41 MPa. Consequently, the thermodynamic phase assemblages show a strong correlation with the compressive strength.

Upon establishing that compressive strength is related to the phase assemblage of cementitious binders, thermodynamic simulations are employed to yield the phase assemblages of all [PC + FA] binders, which correlate with the compressive strength at 3 days. The primary objective of uncovering this correlation is to estimate the degree of reaction of FAs. Due to variations in molecular structures and chemical compositions, it is important to quantitatively estimate the FAs' degree of reaction in PC at 3 days. The degree of reaction for FAs spans a wide range. Generally, partially depolymerized FAs are more reactive compared to fully polymerized FAs. To estimate the degree of reaction of FA at 3 days, thermodynamic simulations of [PC + FA] binders with varying degrees of reaction for FAs—ranging from 1 % to 30 % with 1 % increments—were conducted. The degree of hydration of PCs in [PC + FA] binders at 3 days ranged from 49 % to 56 % (*values obtained from the ratio of short-term and long-term isothermal calorimetry*). The volume fraction

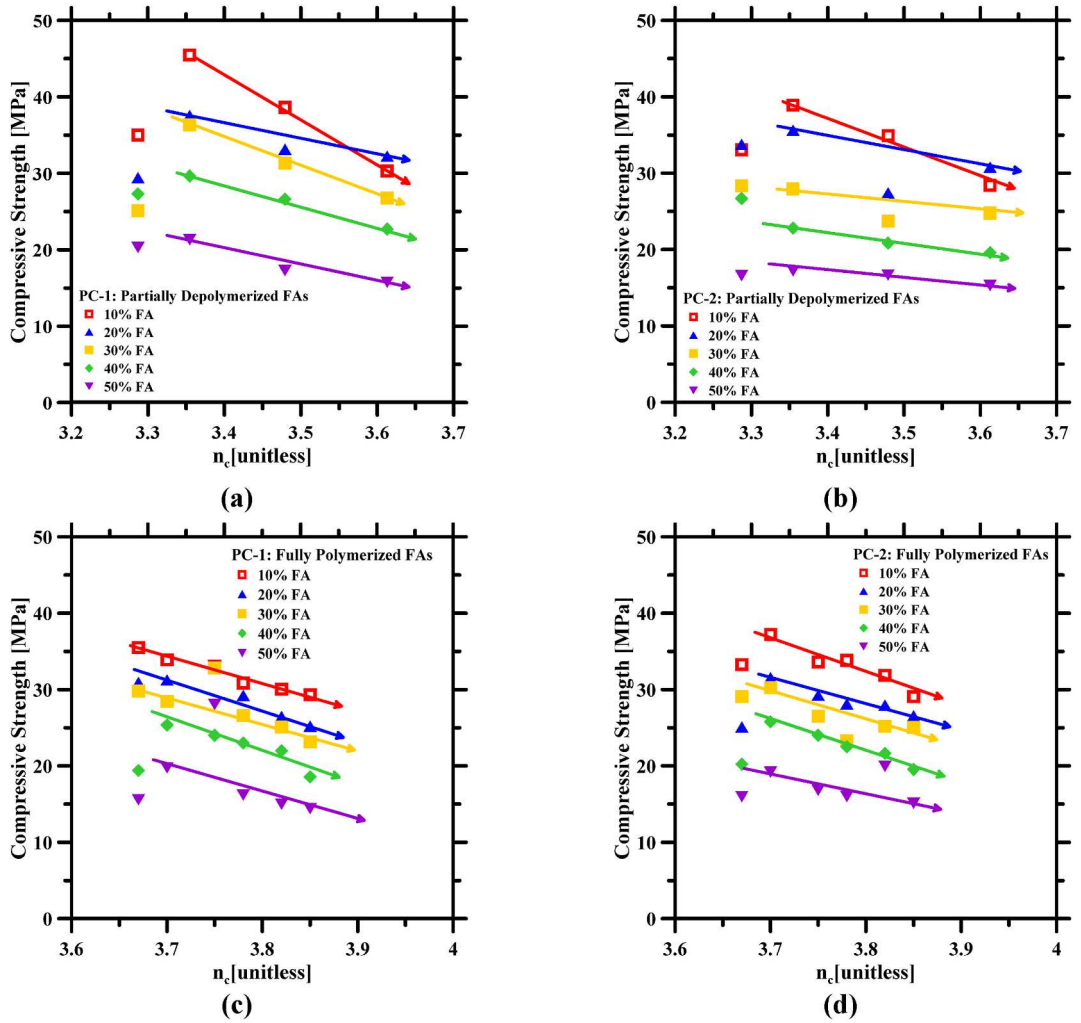

Fig. 4. The compressive strength of [PC + FA] at 3 days corresponding to the *number of constraints*: **(a)** PC-1 substituted by partially depolymerized FAs; **(b)** PC-2 substituted by partially depolymerized FAs; **(c)** PC-1 substituted by fully polymerized FAs; and **(d)** PC-2 substituted by fully polymerized FAs. The solid lines represent the general trend of the correlation.

of all hydrates at 3 days were plotted against the measured compressive strength, and separate plots were generated for each degree of reaction of FA. The best correlation between the volume fraction of hydrates and measured compressive strength, showed in Fig. 6a, indicates that the compressive strength increases monotonically with the volume fraction of hydrates. Based on this correlation, the degree of reaction of FA in each [PC + FA] binder was determined. A key finding from this analysis is that the degree of reaction of a given FA is independent of the chemical composition of PC and the replacement level in the [PC + FA] binder but solely dependent on their chemical composition. The degree of reaction of each FA represents the average value for each PC and each replacement level, with a maximum standard deviation of ~3 %. The degree of reactivity pertaining to all FAs used in this study can be found in Table S3 of the **Supplementary Information**.

The reactivity of FA demonstrates an exponential decrease as the *number of constraints* increases. This is attributed to the fact that FAs with a higher *number of constraints* tend to have a more stable structure, where ions are difficult to dissolve into pore solution. In Fig. 6b, FA-3 (n_c = 3.75) distinctly stands out from the general trend as an outlier. This deviation can be traced back to the limitations inherent in the TCT. It essentially serves as an indirect measure to estimate the amorphous content in FAs. Consequently, there may be instances where certain FAs, despite a high amorphous content, do not conform to the TCT. This can occur in scenarios where FAs have significant silica or aluminate content. Further investigations pertaining to FA-3 will follow in the subsequent sections. Another limitation of TCT is that it does not account for Fe_2O_3, MgO etc. in FAs, even with a substantial amount. It primarily focuses on the C–S-A pseudo ternary systems, and Fe_2O_3 and MgO have no effect on the C–S-A topological network. The presence of Fe_2O_3 and MgO can affect the ettringite, monosulfoaluminate, and hydrotalcite formation in PC hydration, observed in the phase assemblages. However, reactivity of FAs remains unaffected by the presence of these oxides. For a more precise determination of the amorphous content, advanced analytical methods such as Quantitative X-Ray Diffraction could be employed. However, the primary aim of this study

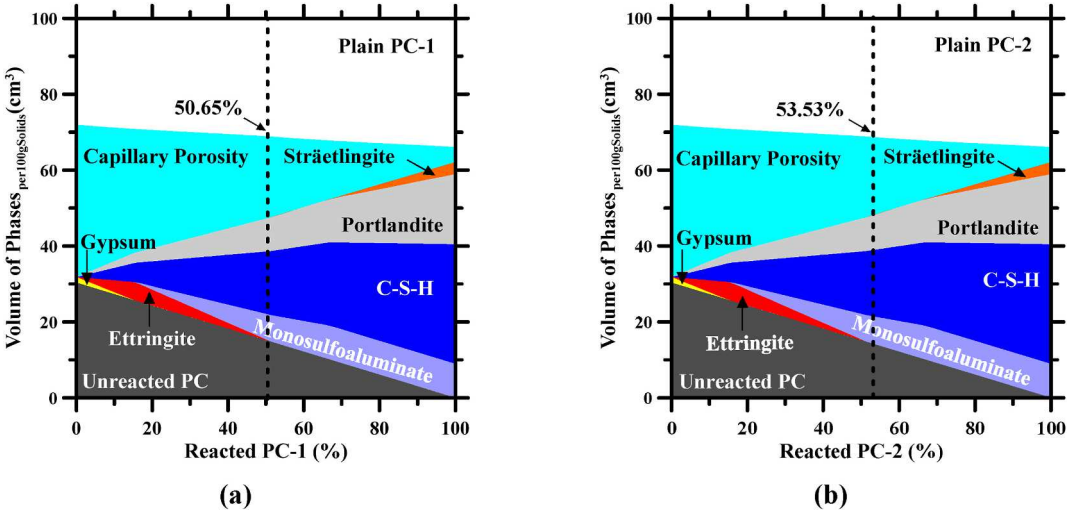

Fig. 5. Equilibrium phase assemblage of: **(a)** plain PC-1; and **(b)** plain PC-2 binders at 3 days as produced by thermodynamic simulations. The vertical dashed line in **(a)** and **(b)** represents the degree of hydration of PC-1 and PC-2, which are 50.65 % and 53.53 % respectively. The value of degree of hydration was obtained from short-term and long-term isothermal calorimetry experiments. In all other thermodynamic simulations of [PC-1 + FA] and [PC-2 + FA] binders, the aforementioned degree of hydration of PC-1 and PC-2 were used.

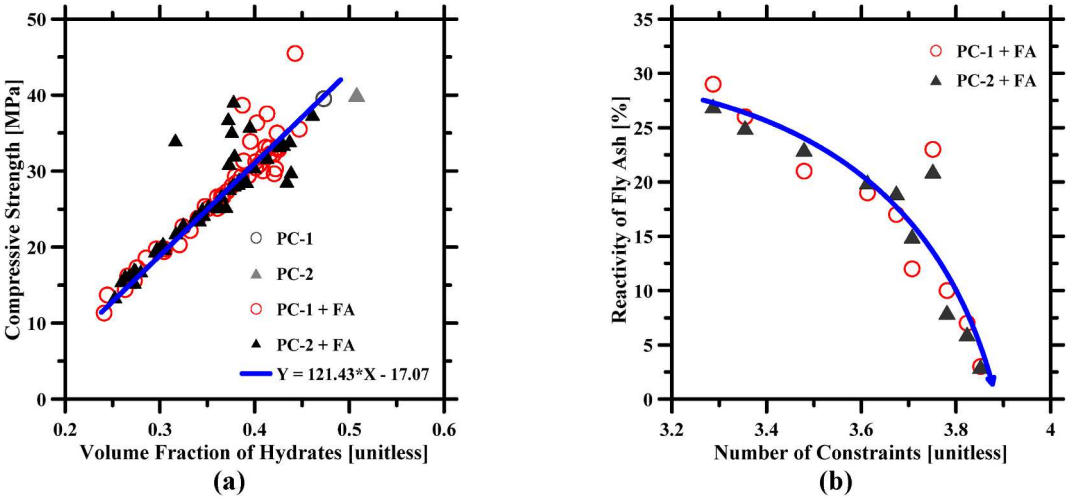

Fig. 6. The correlation between **(a)** volume fraction of hydrates and compressive strength at 3 days; **(b)** *number of constraints* and reactivity of FAs at 3 days. The blue line indicates the general trend of the data points.

is to leverage a cost-effective and simple approach to estimate the reactivity of FA in PC. As such, the presence of these exceptional FA types is acceptable within the scope of this research.

As shown in Fig. 7a, the replacement level of FA-3 does not compromise the compressive strength of [PC + FA-3], even at a 50 % replacement level, where the compressive strength is higher than the strength-dilution line (dashed line). This is due to the high S content in FA-3, which can rapidly react with portlandite and promote the formation of C–S–H. Similar arguments have been discussed in **Section 3.1**. The strong pozzolanic reaction, in turn, counterbalances the compressive strength loss caused by the dilution effect in [PC + FA-3] binders. This can also be observed in the thermodynamic phase assemblages shown in Fig. 7b and **c**. The dashed line indicates the reactivity of FA-3 in both [PC + FA] binders. With 23 % and 21 % reactivity, the abundance of C–S–H clarifies the contribution of FA-3 in the pozzolanic reaction through the consumption of CH. As discussed in **Section 3.1**, the reactivity of FA-3 can also be attributed to its low mean particle size (i.e., d50–8.69 μm) which results in a higher specific surface area for the heterogenous nucleation and growth of C–S–H. The reactivity associated with the high specific surface area of FA-3 has not been quantified in this study. In summary, FA-3 exhibits distinctive behavior in both [PC + FA-3] binders due to its inherent capacity to contribute to the formation of strength-providing phases, unlike other fully polymerized FAs.

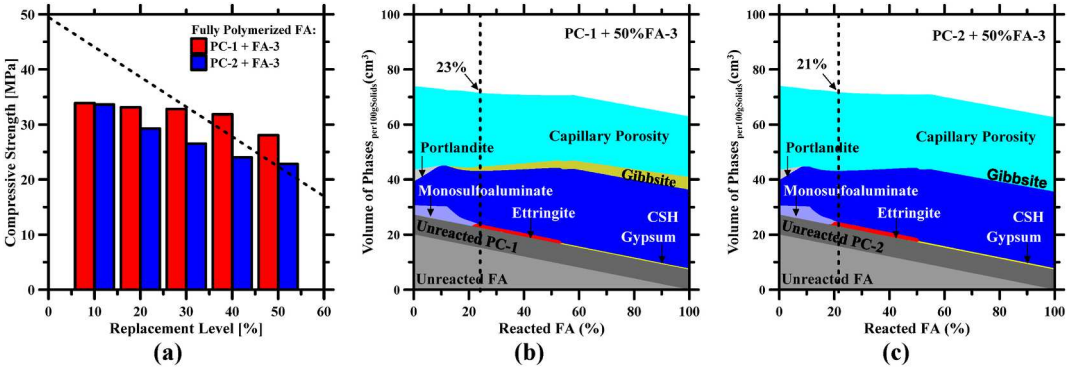

Fig. 7. FA-3, a fully polymerized FA, yielding high compressive strength **(a)** Compressive strength in both [PC + FA-3] binders; Equilibrium phase assemblage of: (b) [PC-1 + 50%$_{mass}$ FA-3]; and (c) [PC-2 + 50%$_{mass}$ FA-3]. In Fig. 7 (a) the dashed line represents the strength dilution when compared to PC-1 and PC-2. In Fig. 7 (b) and 7 (c) the dashed line represents the degree of hydration of FA at 3 days in both PC-1 and PC-2 binders, which was estimated from the correlation between compressive strength and volume fraction of hydrates in the binder. The reactivity of FAs were within ±3 % in both PCs.

4. Conclusions

This paper investigated the influence of the content and chemistry of FAs on the hydration kinetics, compressive strength, and phase assemblage of PCs. Ten FAs with unique chemical compositions and molecular structures were used to partially replace two PCs at 10-to-50%$_{mass}$. Hydration kinetics and compressive strength of [PC + FA] binders at 3 days were measured. The reactivity of FAs is evaluated by using a singular unitless parameter (i.e., *number of constraints*), encompassing the chemical compositions and molecular structures. Furthermore, thermodynamic simulations were employed to predict the phase assemblages of [PC + FA] binders. By analyzing phase assemblages and compressive strength, the degree of reaction of FA at 3 days can be estimated.

The study finds that FAs with low values of *number of constraints* enhance the compressive strength by promoting pozzolanic reactions with PC. FAs with high values of *number of constraints* act as fillers, thereby decreasing the compressive strength. Experimental findings reveal that binders incorporating FA-8 (low *number of constraints*) show the highest compressive strength. In contrast, binders replaced by FA-2 (high *number of constraints*) result in the lowest compressive strength. Notably, FA-3, despite being fully polymerized, demonstrates significant reactivity. It was also observed that all FAs influenced the hydration kinetics and compressive strength of two chemically distinct PCs in a similar manner. Compressive strength of [PC + FA] binders range from 15 to 45 MPa at 3 days. Thermodynamic simulation combining compressive strength measurement has proven to be an effective approach for estimating the fly ash reactivity at 3 days, which vary between 3 % and 29 %. The data also indicate that the reactivity of fly ash diminishes as the number of constraints increases.

This study sheds light on understanding the influence of FAs on the hydration kinetics and compressive strength of substantiable cementitious binders, providing crucial insights for optimizing carbon efficiency compositions while maintaining high performance. The research introduces a cost-effective and simple approach to assess FA reactivity in PC, encouraging their wider adoption in the construction sector. Nonetheless, the simple correlations shown in this study may not fully account for the complex interactions among components in sustainable cementitious binders, highlighting the need for a more advanced model for further optimizing mixture designs and enhancing performance of sustainable cementitious binders. Overall, this investigation marks a significant step toward widely adopting carbon-efficient, and high-performance [PC + FA] binders.

CRediT authorship contribution statement

Rohan Bhat: Writing – original draft, Methodology, Investigation, Formal analysis. **Taihao Han:** Writing – original draft, Investigation, Formal analysis. **Gaurav Sant:** Writing – review & editing, Supervision, Funding acquisition. **Narayanan Neithalath:** Writing – review & editing, Supervision, Funding acquisition. **Aditya Kumar:** Writing – review & editing, Supervision, Funding acquisition, Conceptualization.

Declaration of competing interest

The authors declare that they have no known competing financial interests or personal relationships that could have appeared to influence the work reported in this paper.

Data availability

Data will be made available on request.

Acknowledgements

The authors acknowledge financial support from the Kummer Institute (Missouri S&T) Ignition Grant; the National Science Foundation (NSF-CMMI: 1932690); and the Federal Highway Administration (Award no: 693JJ31950021).

Appendix A. Supplementary data

Supplementary data to this article can be found online at https://doi.org/10.1016/j.jobe.2024.109191.

References

[1] IEA, World Energy Balances: Overview, IEA, Paris, 2021. https://www.iea.org/reports/world-energy-balances-overview.
[2] World coal association, Coal & Electricity, World Coal Association, 2022. https://www.worldcoal.org/coal-facts/coal-electricity.
[3] IEA, Medium-term Coal Market Report 2016, IEA, Paris, 2015. https://www.iea.org/reports/medium-term-coal-market-report-2016.
[4] N.K. Koukouzas, R. Zeng, V. Perdikatsis, W. Xu, E.K. Kakaras, Mineralogy and geochemistry of Greek and Chinese coal fly ash, Fuel 85 (2006) 2301–2309, https://doi.org/10.1016/j.fuel.2006.02.019.
[5] M. Izquierdo, X. Querol, Leaching behaviour of elements from coal combustion fly ash: an overview, Int. J. Coal Geol. 94 (2012) 54–66, https://doi.org/10.1016/j.coal.2011.10.006.
[6] V. Sibanda, S. Ndlovu, G. Dombo, A. Shemi, M. Rampou, Towards the utilization of fly ash as a feedstock for smelter grade alumina production: a review of the developments, J. Sustain. Metall. 2 (2016) 167–184, https://doi.org/10.1007/s40831-016-0048-6.
[7] The Brainy Insights, Fly ash market size by type (Class C and Class F), application (cement and concrete, waste stabilization, oilfield service, fills and embankments, mining, road stabilization and others), in: Global Industry Analysis, Share, Growth, Trends, and Forecast 2023 to 2032, the Brainy Insights, India, 2023. https://www.thebrainyinsights.com/report/fly-ash-market-13417.
[8] C. Belviso, State-of-the-art applications of fly ash from coal and biomass: a focus on zeolite synthesis processes and issues, Prog. Energy Combust. Sci. 65 (2018) 109–135, https://doi.org/10.1016/j.pecs.2017.10.004.
[9] Z.T. Yao, X.S. Ji, P.K. Sarker, J.H. Tang, L.Q. Ge, M.S. Xia, Y.Q. Xi, A comprehensive review on the applications of coal fly ash, Earth Sci. Rev. 141 (2015) 105–121, https://doi.org/10.1016/j.earscirev.2014.11.016.
[10] S. Wang, T. Terdkiatburana, M.O. Tadé, Single and co-adsorption of heavy metals and humic acid on fly ash, Separ. Purif. Technol. 58 (2008) 353–358, https://doi.org/10.1016/j.seppur.2007.05.009.
[11] U. Bhattacharjee, T.C. Kandpal, Potential of fly ash utilisation in India, Energy 27 (2002) 151–166, https://doi.org/10.1016/S0360-5442(01)00065-2.
[12] S.S. Ramya, V.U. Deshmukh, V.J. Khandekar, C. Padmakar, L. SuriNaidu, P.K. Mahore, P.R. Pujari, D. Panaskar, P.K. Labhasetwar, V.V.S.G. Rao, Assessment of impact of ash ponds on groundwater quality: a case study from Koradi in Central India, Environ. Earth Sci. 69 (2013) 2437–2450, https://doi.org/10.1007/s12665-012-2071-7.
[13] B. Prasad, K.K.R. Mondal, Environmental impact of manganese due to its leaching from coal fly ash, J. Environ. Sci. Eng. 51 (2009) 27–32.
[14] L. Long, X. Jiang, G. Lv, Q. Chen, X. Liu, Y. Chi, J. Yan, X. Zhao, L. Kong, Q. Qiu, Comparison of MSWI fly ash from grate-type and circulating fluidized bed incinerators under landfill leachate corrosion scenarios: the long-term leaching behavior and speciation of heavy metals, Environ. Sci. Pollut. Control Ser. 29 (2022) 15057–15067, https://doi.org/10.1007/s11356-021-16618-z.
[15] D. Dabrowska, W. Rykala, V. Nourani, Causes, types and consequences of municipal waste landfill fires—literature Review, Sustainability 15 (2023) 5713, https://doi.org/10.3390/su15075713.
[16] H.M. Omar, S. Rohani, Removal of CO_2 from landfill gas with landfill leachate using absorption process, Int. J. Greenh. Gas Control 58 (2017) 159–168, https://doi.org/10.1016/j.ijggc.2017.01.011.
[17] R.N.K. Nutini Janet Rickabaugh, Martha Lambert, L. David, Control of methane from municipal solid waste landfills by injection of lime and flyash, in: Proceedings of the 43rd Industrial Waste Conference May 1988, 1989 Purdue University, CRC Press.
[18] X. Liu, Q. Song, Y. Tang, W. Li, J. Xu, J. Wu, F. Wang, P.C. Brookes, Human health risk assessment of heavy metals in soil–vegetable system: a multi-medium analysis, Sci. Total Environ. (2013) 530–540 https://doi.org/10.1016/j.scitotenv.2013.06.064, 463–464.
[19] S.K. Adhikary, A. D'Angelo, V. Viola, M. Catauro, P. Perumal, Alternative construction materials from industrial side streams: are they safe? Energ. Ecol. Environ. (2023), https://doi.org/10.1007/s40974-023-00298-1.
[20] A. Dowling, J. O'Dwyer, C.C. Adley, Lime in the limelight, J. Clean. Prod. 92 (2015) 13–22, https://doi.org/10.1016/j.jclepro.2014.12.047.
[21] F. Schorcht, Best Available Techniques (BAT) reference document for the production of cement, lime and magnesium oxide: industrial emissions directive 2010/75/EU:(Integrated Pollution Prevention and Control), EU Science Hub - European Commission, https://ec.europa.eu/jrc/en/publication/reference-reports/best-available-techniques-bat-reference-document-production-cement-lime-and-magnesium-oxide, 2013. (Accessed 15 April 2020).
[22] M.M. Miller, Lime, United States Geological Survey, 2012 Minerals Yearbook, 2013.
[23] Growing at a slower pace, world population is expected to reach 9.7 billion in 2050 and could peak at nearly 11 billion around 2100 | UN DESA | United Nations Department of Economic and Social Affairs, https://www.un.org/development/desa/en/news/population/world-population-prospects-2019.html.
[24] International energy agency, cement technology roadmap, Carbon Emissions Reductions up to 2050, OECD, 2009, https://doi.org/10.1787/9789264088061-en.
[25] R. Kajaste, M. Hurme, Cement industry greenhouse gas emissions – management options and abatement cost, J. Clean. Prod. 112 (2016) 4041–4052, https://doi.org/10.1016/j.jclepro.2015.07.055.
[26] N. Sahoo, A. Kumar, Samsher, Review on energy conservation and emission reduction approaches for cement industry, Environmental Development 44 (2022) 100767, https://doi.org/10.1016/j.envdev.2022.100767.
[27] E. Worrell, N. Martin, L. Price, Potentials for energy efficiency improvement in the US cement industry, Energy 25 (2000) 1189–1214, https://doi.org/10.1016/S0360-5442(00)00042-6.
[28] S. Griffiths, B.K. Sovacool, D.D. Furszyfer Del Rio, A.M. Foley, M.D. Bazilian, J. Kim, J.M. Uratani, Decarbonizing the cement and concrete industry: a systematic review of socio-technical systems, technological innovations, and policy options, Renew. Sustain. Energy Rev. 180 (2023) 113291, https://doi.org/10.1016/j.rser.2023.113291.
[29] J. Lapeyre, A. Kumar, Influence of pozzolanic additives on hydration mechanisms of tricalcium silicate, J. Am. Ceram. Soc. 101 (2018) 3557–3574, https://doi.org/10.1111/jace.15518.
[30] T. Oey, A. Kumar, J.W. Bullard, N. Neithalath, G. Sant, The Filler Effect: the influence of filler content and surface area on cementitious reaction rates, J. Am. Ceram. Soc. 96 (2013) 1978–1990, https://doi.org/10.1111/jace.12264.
[31] A. Kumar, T. Oey, S. Kim, D. Thomas, S. Badran, J. Li, F. Fernandes, N. Neithalath, G. Sant, Simple methods to estimate the influence of limestone fillers on reaction and property evolution in cementitious materials, Cement Concr. Compos. 42 (2013) 20–29, https://doi.org/10.1016/j.cemconcomp.2013.05.002.
[32] Standard specification for coal fly ash and raw or calcined natural pozzolan for use in concrete, https://www.astm.org/c0618-19.html.
[33] R. Bhat, T. Han, S. Akshay Ponduru, A. Reka, J. Huang, G. Sant, A. Kumar, Predicting compressive strength of alkali-activated systems based on the network topology and phase assemblages using tree-structure computing algorithms, Construct. Build. Mater. 336 (2022) 127557, https://doi.org/10.1016/j.conbuildmat.2022.127557.
[34] T. Han, R. Bhat, S.A. Ponduru, A. Sarkar, J. Huang, G. Sant, H. Ma, N. Neithalath, A. Kumar, Deep learning to predict the hydration and performance of fly ash-containing cementitious binders, Cement Concr. Res. 165 (2023) 107093, https://doi.org/10.1016/j.cemconres.2023.107093.
[35] A. Oner, S. Akyuz, R. Yildiz, An experimental study on strength development of concrete containing fly ash and optimum usage of fly ash in concrete, Cement Concr. Res. 35 (2005) 1165–1171, https://doi.org/10.1016/j.cemconres.2004.09.031.
[36] K. De Weerdt, M.B. Haha, G. Le Saout, K.O. Kjellsen, H. Justnes, B. Lothenbach, Hydration mechanisms of ternary Portland cements containing limestone powder and fly ash, Cement Concr. Res. 41 (2011) 279–291, https://doi.org/10.1016/j.cemconres.2010.11.014.
[37] S.C. Kou, C.S. Poon, D. Chan, Influence of fly ash as cement replacement on the properties of recycled aggregate concrete, J. Mater. Civ. Eng. 19 (2007) 709–717, https://doi.org/10.1061/(ASCE)0899-1561(2007)19.9709.
[38] G.L. Golewski, Examination of water absorption of low volume fly ash concrete (LVFAC) under water immersion conditions, Mater. Res. Express 10 (2023) 085505, https://doi.org/10.1088/2053-1591/acedef.

[39] G.L. Golewski, The role of pozzolanic activity of siliceous fly ash in the formation of the structure of sustainable cementitious composites, Sustainable Chemistry 3 (2022) 520–534, https://doi.org/10.3390/suschem3040032.
[40] G.L. Golewski, Assessing of water absorption on concrete composites containing fly ash up to 30 % in regards to structures completely immersed in water, Case Stud. Constr. Mater. 19 (2023) e02337, https://doi.org/10.1016/j.cscm.2023.e02337.
[41] G.L. Golewski, The effect of the addition of coal fly ash (cfa) on the control of water movement within the structure of the concrete, Materials 16 (2023) 5218, https://doi.org/10.3390/ma16155218.
[42] G.L. Golewski, Concrete Composites Based on quaternary blended cements with a reduced width of initial microcracks, Appl. Sci. 13 (2023) 7338, https://doi.org/10.3390/app13127338.
[43] M.B. Haha, K. De Weerdt, B. Lothenbach, Quantification of the degree of reaction of fly ash, Cement Concr. Res. 40 (2010) 1620–1629, https://doi.org/10.1016/j.cemconres.2010.07.004.
[44] D. Glosser, P. Suraneni, O.B. Isgor, W.J. Weiss, Estimating reaction kinetics of cementitious pastes containing fly ash, Cement Concr. Compos. 112 (2020) 103655, https://doi.org/10.1016/j.cemconcomp.2020.103655.
[45] S. Li, D.M. Roy, A. Kumar, Quantatative determination of pozzolanas in hydrated systems of cement or $Ca(OH)_2$ with fly ash or silica fume, Cement Concr. Res. 15 (1985) 1079–1086, https://doi.org/10.1016/0008-8846(85)90100-0.
[46] Standard Test method for compressive strength of hydraulic cement mortars (Using 2-in. or [50 mm] Cube Specimens), https://www.astm.org/c0109_c0109m-20b.html.
[47] D. Kulik, F. Winnefeld, A. Kulik, G. Miron, B. Lothenbach, CemGEMS – an Easy-To-Use Web Application for Thermodynamic Modelling of Cementitious Materials, vol. 6, 2021, pp. 36–52, https://doi.org/10.21809/rilemtechlett.2021.140.
[48] Q. Zeng, K. Li, T. Fen-chong, P. Dangla, Determination of cement hydration and pozzolanic reaction extents for fly-ash cement pastes, Construct. Build. Mater. 27 (2012) 560–569, https://doi.org/10.1016/j.conbuildmat.2011.07.007.
[49] M. Narmluk, T. Nawa, Effect of fly ash on the kinetics of Portland cement hydration at different curing temperatures, Cement Concr. Res. 41 (2011) 579–589, https://doi.org/10.1016/j.cemconres.2011.02.005.
[50] N. Schwarz, N. Neithalath, Influence of a fine glass powder on cement hydration: comparison to fly ash and modeling the degree of hydration, Cement Concr. Res. 38 (2008) 429–436, https://doi.org/10.1016/j.cemconres.2007.12.001.
[51] J. Lapeyre, H. Ma, A. Kumar, Effect of particle size distribution of metakaolin on hydration kinetics of tricalcium silicate, J. Am. Ceram. Soc. 102 (2019) 5976–5988, https://doi.org/10.1111/jace.16467.
[52] A. Quennoz, K.L. Scrivener, Hydration of C_3A–gypsum systems, Cement Concr. Res. 42 (2012) 1032–1041, https://doi.org/10.1016/j.cemconres.2012.04.005.
[53] T. Matschei, B. Lothenbach, F.P. Glasser, Thermodynamic properties of portland cement hydrates in the system $CaO–Al_2O_3–SiO_2–CaSO_4–CaCO_3–H_2O$, Cement Concr. Res. 37 (2007) 1379–1410, https://doi.org/10.1016/j.cemconres.2007.06.002.
[54] B. Lothenbach, T. Matschei, G. Möschner, F.P. Glasser, Thermodynamic modelling of the effect of temperature on the hydration and porosity of Portland cement, Cement Concr. Res. 38 (2008) 1–18, https://doi.org/10.1016/j.cemconres.2007.08.017.
[55] D.P. Bentz, Three-dimensional computer simulation of portland cement hydration and microstructure development, J. Am. Ceram. Soc. 80 (1997) 3–21, https://doi.org/10.1111/j.1151-2916.1997.tb02785.x.
[56] X. Chen, S. Wu, J. Zhou, Influence of porosity on compressive and tensile strength of cement mortar, Construct. Build. Mater. 40 (2013) 869–874, https://doi.org/10.1016/j.conbuildmat.2012.11.072.
[57] C. Lian, Y. Zhuge, S. Beecham, The relationship between porosity and strength for porous concrete, Construct. Build. Mater. 25 (2011) 4294–4298, https://doi.org/10.1016/j.conbuildmat.2011.05.005.
[58] S. Popovics, New formulas for the prediction of the effect of porosity on concrete strength, J. Am. Concr. Inst. 82 (1985) 136–146.
[59] L. Li, M. Aubertin, A general relationship between porosity and uniaxial strength of engineering materials, Can. J. Civ. Eng. 30 (2003) 644–658, https://doi.org/10.1139/l03-012.
[60] D.M. Roy, G.R. Gouda, Porosity-strength relation in cementitious materials with very high strengths, J. Am. Ceram. Soc. 56 (1973) 549–550, https://doi.org/10.1111/j.1151-2916.1973.tb12410.x.
[61] I. Mehdipour, A. Kumar, K.H. Khayat, Rheology, hydration, and strength evolution of interground limestone cement containing PCE dispersant and high volume supplementary cementitious materials, Mater. Des. 127 (2017) 54–66, https://doi.org/10.1016/j.matdes.2017.04.061.
[62] B. Lothenbach, G. Le Saout, E. Gallucci, K. Scrivener, Influence of limestone on the hydration of Portland cements, Cement Concr. Res. 38 (2008) 848–860, https://doi.org/10.1016/j.cemconres.2008.01.002.
[63] D. Bentz, T. Barrett, I. De la Varga, W. Weiss, Relating compressive strength to heat release in mortars, Advances in Civil Engineering Materials 1 (2012) 14, https://doi.org/10.1520/ACEM20120002.
[64] S.W. Dean, D.P. Bentz, A. Durán-Herrera, D. Galvez-Moreno, Comparison of ASTM C311 strength activity index testing versus testing based on constant volumetric proportions, J. ASTM Int. (JAI) 9 (2012) 104138, https://doi.org/10.1520/JAI104138.
[65] S.E. Chidiac, F. Moutassem, F. Mahmoodzadeh, Compressive strength model for concrete, Mag. Concr. Res. 65 (2013) 557–572, https://doi.org/10.1680/macr.12.00167.
[66] K. Svinning, A. Høskuldsson, H. Justnes, Prediction of compressive strength up to 28 days from microstructure of Portland cement, Cement Concr. Compos. 30 (2008) 138–151, https://doi.org/10.1016/j.cemconcomp.2007.05.016.
[67] M.A. Uddin, M. Jameel, H.R. Sobuz, N.M.S. Hasan, M.S. Islam, K.M. Amanat, The effect of curing time on compressive strength of composite cement concrete, Appl. Mech. Mater. 204–208 (2012) 4105–4109. https://doi.org/10.4028/www.scientific.net/AMM.204-208.4105.
[68] T.C. Fu, W. Yeih, J.J. Chang, R. Huang, The influence of aggregate size and binder material on the properties of pervious concrete, Adv. Mater. Sci. Eng. 2014 (2014) e963971, https://doi.org/10.1155/2014/963971.
[69] F. Hong, M. Wang, B. Dong, X. Diao, X. Zhang, K. Pang, Y. Zhang, D. Hou, Molecular insight into the pozzolanic reaction of metakaolin and calcium hydroxide, Langmuir 39 (2023) 3601–3609, https://doi.org/10.1021/acs.langmuir.2c03115.
[70] I. Soroka, N. Setter, The effect of fillers on strength of cement mortars, Cement Concr. Res. 7 (1977) 449–456, https://doi.org/10.1016/0008-8846(77)90073-4.